

MOCVD Buffer and Superconducting Layers on Non-Magnetic Biaxially Textured Tape for Coated Conductor Fabrication

Andrey R. Kaul, Sergey V. Samoilenkov, Vadim A. Amelichev, Andrey V. Blednov, Anton A. Kamenev, Alexey S. Mankevich, Anton V. Markelov, Artem M. Makarevich, Alexander E. Shchukin, Vladislav S. Kalitka, Alexander A. Adamenkov, Vsevolod N. Chepikov, Andrey T. Matveev, Lidia I. Burova, Alexey I. Kuchaev, and Andrey P. Vavilov

Abstract—In this article, we present recent developments in the metal-organic chemical vapor deposition (MOCVD) route to coated conductor fabrication made at SuperOx. Two new buffer layer architectures on nonmagnetic Ni-Cr-W biaxially textured substrates are described. With the use of these architectures we have achieved critical currents in the range of 100–140 A/cm-width for the fully MOCVD produced coated conductors on Ni-Cr-W in the reel-to-reel mode. We have also demonstrated over 10-m-long MOCVD-high temperature superconductor tapes on the ion beam assisted deposition templates with I_c exceeding 300 A/cm-width.

Index Terms—Coated conductors, critical current, metal-organic chemical vapor deposition (MOCVD), Ni-Cr-W, RABiTS.

I. INTRODUCTION

CHEMICAL deposition methods promise cost-effective routes to manufacture coated conductors. These methods enable high throughput through the increase of deposition area with moderate capital investment. Even though chemical deposition processes are in general more difficult to control as compared to physical deposition processes, their amenability to scale up may give them significant advantages in the future, when thousands of kilometers of HTS wire are to be produced to fulfill the demand of the application industry. The contemporary commercial HTS wire is produced with the help of chemical approaches: MOCVD [1], [2] and MOD [3], [4].

SuperOx company was founded in Russia in 2006 with the goal to develop economical manufacturing technology of the second generation HTS tapes based on biaxially textured metal templates and the metal-organic chemical vapor deposition (MOCVD) method to grow all oxide layers.

Manuscript received October 9, 2012; accepted December 23, 2012. Date of publication January 4, 2013; date of current version February 1, 2013. This work was partly supported by the Ministry of Education and Science of the Russian Federation under Contract 16.523.11.3008.

A. R. Kaul, A. M. Makarevich, A. E. Schchukin, A. A. Adamenkov, and V. N. Chepikov are with SuperOx, 143082 Moscow region, Odintsovskii district, Russia. They are also with the Chemistry Department, Moscow State University, 119991 Moscow, Russia.

S. V. Samoilenkov is with SuperOx, 143082 Moscow region, Odintsovskii district, Russia. He is also with the Institute of High Temperature RAS, 125412 Moscow, Russia (e-mail: s.samoilenkov@gmail.com).

V. A. Amelichev, A. V. Blednov, A. A. Kamenev, A. S. Mankevich, A. V. Markelov, V. S. Kalitka, A. T. Matveev, L. I. Burova, A. I. Kuchaev, and A. P. Vavilov are with SuperOx, 143082 Moscow region, Odintsovskii district, Russia.

Digital Object Identifier 10.1109/TASC.2013.2237932

The main features of our approach are the use of biaxially textured Ni-Cr-W tape, which is non-magnetic at 77 K, and the MOCVD method to deposit all oxide layers of the coated conductor, including the buffer and the HTS layers. In this paper we review the progress we have made recently along this path.

II. EXPERIMENTAL

A. Biaxially Textured Metal Tape

The composition of the alloy to prepare biaxially textured tape was Ni-9.2 at.%Cr-2.4 at.%W. Chromium was added to the more conventional Ni-W alloy in order to suppress its ferromagnetism. In general, an increase of the doping level leads to an increase of the mechanical strength and to a decrease of the Curie point and the content of cubic texture. Therefore, an alloy composition delivering a reasonable compromise among these properties needs to be found. The above composition was selected as one possessing an optimal combination of the Curie point of about 50 K and the achievable texture as high as 99% [5].

The alloy vacuum casting, forging and cold rolling were performed at a contracted metallurgical factory. The initial weight of the alloy was above 300 kg. The strip was cold rolled in multiple steps without any intermediate annealing, with the reduction per step not exceeding 10% of the thickness and the speed not exceeding 20 m/min. The total thickness reduction was in the 99.0–99.5% range. The cross section of a single strip was typically 80 micrometers \times 100 mm with a strip length up to 1.4 km.

The resulting cold-rolled tape was slit into 10 mm wide stripes, ultrasonically washed, annealed and electropolished in a specially designed reel-to-reel equipment.

Alongside with the non-magnetic RABiTS, we also used procured Hastelloy templates with biaxially aligned layers prepared through the ion beam assisted deposition (IBAD) route.

B. MOCVD of Buffer and Superconducting Layers

The MOCVD growth of oxide buffer and HTS layers was performed in four lab scale reel-to-reel systems, which were designed, constructed and put into operation at SuperOx.

Volatile chelate complexes of corresponding metals based on 2,2,6,6-tetramethylheptanedione-3,5 (thd) were used as

precursors. The precursors were synthesized in-house at our company, thus ensuring the lowest possible cost of raw materials for MOCVD. We developed new synthetic procedures to increase the yield of volatile compounds, e.g., a one-stage reaction for $\text{Ba}(\text{thd})_2 \cdot 2\text{Phen}$ production, providing the yield over 95% and reducing the time of synthesis down to 2 hours [6].

We succeeded in the deposition of epitaxial magnesia directly on the Ni-Cr-W substrate tape. Magnesium oxide provides an excellent combination of properties desired for the first buffer layer, including high tendency to (001)-oriented growth, very low oxygen diffusion and excellent chemical compatibility with the Ni-Cr-W alloy.

Additional buffer layers were required to provide appropriate template for the HTS growth. For Ni-Cr-W substrate we developed two alternative buffer layer architectures, both of which had in common the first MgO layer: (1) epitaxial SrF_2 layer on MgO with subsequent CeO_2 or other fluorite-type oxide [7], [8] and (2) epitaxial BaZrO_3 layer on MgO [9].

We used YBCO for the superconductor layer. For the MOCVD growth of the YBCO layer, we used argon as a carrier gas and oxygen as a reactant gas. The growth was performed in the temperature range of 780–850 °C and at $p(\text{O}_2)$ of 1–2 mbar. The film thickness varied in the range of 1–2 micrometers, whereas the local growth rate was about 8 $\mu\text{m}/\text{h}$.

C. Metal Layers and Oxidation

Silver layer was grown on top of the HTS layer in a DC magnetron sputtering system of our original design equipped with a 6 kW power source. A multi-pass helical tape handling assembly with 4 tape lanes was employed for a more effective use of the 100 mm-diameter silver target disc. No active heating or cooling of the tape was performed during the deposition; we observed however that during the growth the temperature in the deposition zone rose to approximately 100 °C. The process gas was argon and the sputtering was performed in the pressure range of $3 - 10 \times 10^{-3}$ mbar. The tape speed was typically 25 m/h resulting in a 1 μm thick silver coating. After silver deposition the tapes were annealed in flowing oxygen at 450 °C for 1 hour to oxygenate the HTS layer.

Finally, the copper stabilizing layer was deposited using the standard electrodeposition technique at room temperature in a specially designed reel-to-reel system. This compact device operating at the tape speed of 18 m/h provided 20 μm of uniform copper coating on both sides of the HTS tape. The electrodeposited copper ensures electrical stabilization and protection of the product.

D. Critical Current Measurements

Both transport and magnetic measurements were performed in liquid nitrogen at 77.3 K. The critical current of the HTS tapes was measured on the full tape width by direct transport measurements on stationary samples in self field and by Hall sensor imaging of the trapped magnetic field on continuously moving samples using a reel-to-reel system of our original design (the measurement principle is described in [10]). The

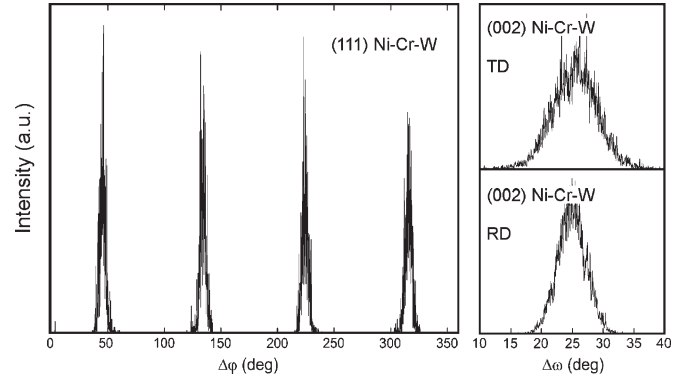


Fig. 1. XRD texture analysis of the Ni-Cr-W tape produced in reel-to-reel mode.

measurements of 2D critical current distribution were performed on 4, 10 and 12 mm-wide tapes at the tape speed up to 90 m/h.

E. Analytical Methods

Texture characteristics of the samples were routinely measured with Rigaku SmartLab X-ray diffractometer and electron backscattering surface diffraction using Jeol 840A SEM with Channel 5 HKL EBSD system. The surface morphology was studied with Carl Zeiss EVO50 and Leo Supra microscopes. Surface roughness was measured with NT-MDT Aura NTEGRA AFM device.

III. RESULTS AND DISCUSSION

A. Biaxially Textured Ni-Cr-W Metal Tape

We characterized the texture of the Ni-Cr-W tape with the EBSD and XRD techniques. Typically, 97%–99% of the alloy grains were oriented within the 10° misorientation margin from the ideal cube orientation, with the following texture parameters: $\Delta\omega_{\text{RD}} = 5.2^\circ$, $\Delta\omega_{\text{TD}} = 8.7^\circ$, $\Delta\varphi_{\text{TRUE}} = 5.6^\circ$ (RD stands for rolling direction, TD for transverse direction, and $\Delta\varphi_{\text{TRUE}}$ values were determined following the procedure described in [11]) (Fig. 1).

The surface roughness of the tapes determined on $5 \times 5 \mu\text{m}^2$ AFM scans was below 5 nm, although still slightly higher than the values typically reported for commercially available Ni-5at.% W tapes carefully rolled with mirror-finish rolls. However, we regard electropolishing of RABiTS as beneficial, since it reduces the requirements to rolling facility and also effectively removes grooving at grain boundaries, which can be 100 nm deep in the otherwise smoother unpolished tapes.

Even though we have not studied this issue in details, the mechanical properties of textured Ni-Cr-W tape were found to be very similar to that of conventional Ni-5at.%W alloy, with the difference not exceeding 10% of corresponding values.

B. MOCVD of Buffer Layers on Ni-Cr-W Metal Tape

The thickness of our MgO layers was 120–130 nm. The texture of the MgO buffer layer was found to replicate that of the metal substrate with $\Delta\omega_{\text{RD}} = 6.0^\circ$, $\Delta\omega_{\text{TD}} = 9.0^\circ$, and

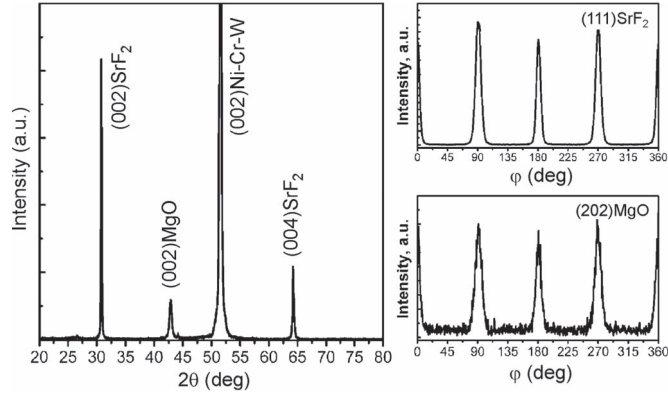


Fig. 2. XRD texture analysis of the SrF₂/MgO/Ni-Cr-W structure.

$\Delta\varphi_{\text{TRUE}} = 5.2^\circ$. We have not observed the effect of texture improvement in our case. MgO was found to grow on the Ni-Cr-W surface with pure cube-on-cube orientation. According to the SEM observations, the average MgO grain size was about 200–300 nm. No cracking of the MgO layer was found.

The HTS layers grown directly on the MgO surface by the majority of deposition techniques demonstrate poor in-plane texture, one of the rare exceptions being epitaxial YBCO/MgO films grown by the RCE method [12]. Either dimensional or structural mismatch between the YBCO and MgO lattices needs to be reduced by using appropriate cap layers, in order to attain good superconducting properties. We developed two efficient buffer layer architectures on top of MgO that resolve this issue.

The first architecture is based on the use of strontium fluoride (SrF₂) layer, which possesses fluorite-type structure and has low lattice mismatch with MgO (−1.7%). It allows for the growth of epitaxial heterostructures with the following epitaxial relations:

$$(001)[110]\text{SrF}_2 // (001)[100]\text{MgO} // (001)[100]\text{Ni-Cr-W}$$

Subsequent deposition of ceria, yttria or any other fluorite-type oxide cap layer on top of SrF₂ results in a suitable template for YBCO growth.

To grow SrF₂, we developed two alternative MOCVD routes described in detail in [7], [8]. In the reel-to-reel mode we achieved high quality SrF₂ layers using fluorinated volatile precursors and water as reactant gas at a deposition temperature of 300 °C (Fig. 2). The process is very fast with the tape speed of 15 m/h within the deposition zone, which is only 10 cm long.

The other architecture is based on the use of BaZrO₃ (BZO) perovskite as a cap layer reducing the structural difference of the MgO layer with YBCO. This layer was grown by MOCVD at 800 °C at the tape speed of 15 m/h resulting in a 100 nm thick BZO film. The lattice parameters of BZO and MgO are very close, which means that the dimensional mismatch between YBCO and the BZO buffer layer remains as high as it was with MgO. However, the YBCO layer demonstrated perfect cube-on-cube in-plane alignment with the BZO cap layer that we believe is because of the closely related perovskite-type structures of these two compounds. Additionally, we observed significantly lower content of *a*-axis orientation in the YBCO layers on the BZO cap in comparison with the YBCO films

TABLE I
PROPERTIES OF THE MOCVD YBCO LAYERS ON VARIOUS TEMPLATES

Substrate	$\Delta\omega_{\text{RD}}$ for buffer (deg)	$\Delta\omega_{\text{RD}}$ for (005)YBCO (deg)	End-to-end I_c (A/cm)	Piece length (m)
Y ₂ O ₃ /SrF ₂ / /MgO/NiCrW	6	5-6	100	1
BaZrO ₃ / /MgO/NiCrW	6	1.3-1.8	140	1
LMO/.. IBAD-MgO/.. Hastelloy	2	1.3	250-310	10

grown on perovskites with closer lattice match to YBCO, such as LMO or STO [9]. The reduced *a*-axis growth leads to improved critical current.

C. MOCVD HTS Layers on Various Templates

The typical characteristics of the YBCO layers grown by reel-to-reel MOCVD on various templates are summarized in Table I.

It is interesting to note that the YBCO films on the BZO buffer demonstrated a very good out-of-plane alignment (FWHM values of XRD rocking curves were as low as 1.3°), much better than that of the original RABiTS tape and the buffers. It means that the YBCO (00*l*) planes are better aligned than those of the Ni-Cr-W tape. We suppose that some peculiarities of the YBCO growth on the BZO (001) surface are responsible for this behavior. Briefly, the large lattice mismatch (−8.1%) increases the energy of the YBCO/BZO interface and makes it possible for the YBCO (00*l*) planes to “overflow” 1-unit-cell high steps on the BZO surface without formation of anti-phase boundaries. This leads to the fact that the YBCO (00*l*) planes are better aligned with the physical substrate surface than with the crystallographic BZO (00*l*) planes. Such a behavior is unlikely when the underlying cap layer (such as LMO or CeO₂) has a good lattice match with YBCO and forms a coherent low-energy interface. More experimental data including the transmission electron microscopy observations of the YBCO/BZO interface will be published elsewhere.

The properties of the YBCO layers grown on the IBAD-based templates were generally better than those on the Ni-Cr-W RABiTS (Table I). This fact reflects the much better crystal alignment of the IBAD templates (typically, $\Delta\omega < 2^\circ$, $\Delta\varphi_{\text{TRUE}} < 4^\circ$), but one must also bear in mind that the MOCVD buffer layers on non-magnetic RABiTS are still under development and their quality is likely to increase in the course of further research.

D. Uniformity of the Critical Current Distribution

The critical current distribution in the HTS tapes was studied by non-contact 2D mapping using the reel-to-reel system developed by SuperOx in collaboration with Moscow Engineering Physics Institute [Fig. 3(a)]. The distribution of the trapped field in the moving tape was measured by the array of nine Hall sensors. Critical current was determined by the inversion of the Biot-Savart-Laplace equation [10].

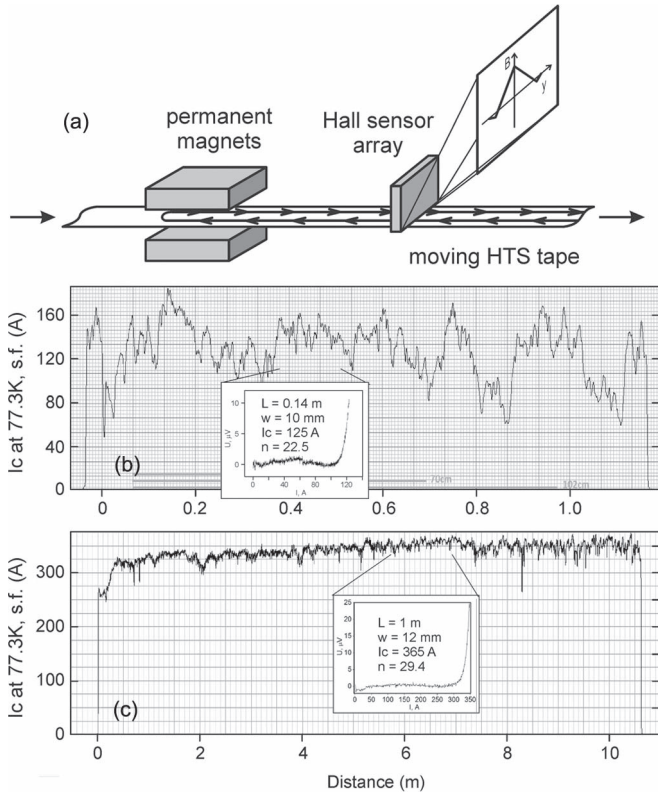


Fig. 3. (a) Principle of the noncontact critical current measurement. Critical current distribution over the length of a YBCO sample (b) on the BZO/MgO/Ni-Cr-W template and (c) on the IBAD-based template. The insets to Fig. 3(b) and 3(c) show the I - V curves obtained by direct transport measurements of selected sections of the entire tapes.

The n -values determined from transport measurements were in the range of 25–35. Overall, we found that the tapes on the IBAD templates showed better I_c uniformity over length than the tapes on the RABiTS templates [Fig. 3(b) and (c)]. We believe that with further process development we will attain higher and more uniform critical currents of the RABiTS-based tapes.

IV. CONCLUSION

We have been developing a complete technological path to coated conductor fabrication from a metal alloy production to

the copper-finished HTS wire. Our approach is based on the use of non-magnetic biaxially textured substrate tapes made from the Ni-Cr-W alloy and of the scalable MOCVD process for the deposition of oxide layers. The use of new buffer layer architectures allowed us to obtain encouraging results with I_c (77.3 K, s.f.) of 100–140 A/cm-width. Further optimization of the processes is on the way, aimed at improving current-carrying characteristics of the coated conductor tapes and their uniformity. Using the developed MOCVD approach we prepared several 10 m long tapes on the IBAD-based templates with I_c (77.3 K, s.f.) exceeding 300 A/cm-width.

REFERENCES

- [1] Y. Chen *et al.*, "Progress in performance improvement and new research areas for cost reduction of 2G HTS wires," *IEEE Trans. Appl. Supercond.*, vol. 21, pp. 3049–3054, 2011.
- [2] Y. Chen, "High performance 2G wires: From R&D to pilot-scale manufacturing," *IEEE Trans. Appl. Supercond.*, vol. 19, pp. 3225–3230, 2009.
- [3] M. W. Rupich, "Advanced development of TFA-MOD coated conductors," *Phys. C*, vol. 471, pp. 919–923, 2011.
- [4] M. W. Rupich, "Advances in second generation high temperature superconducting wire manufacturing and R&D at American Superconductor Corporation," *Supercond. Sci. Technol.*, vol. 23, p. 014015, 2010.
- [5] A. R. Kaul *et al.*, "Development of non-magnetic biaxially textured tape and MOCVD processes for coated conductor fabrication," *Phys. Proc.*, vol. 36, pp. 1434–1439, 2012.
- [6] S. V. Samoilenkov, O. V. Kotova, and N. P. Kuz'mina, "Synthesis of mixed-ligand alkali earth element dipivaloymethanates with *o*-phenanthroline," (in Russian), *Russ. J. Coord. Chem.*, vol. 35, pp. 793–797, 2009.
- [7] A. V. Blednov, O. Y. Gorbenko, S. V. Samoilenkov, V. A. Amelichev, V. A. Lebedev, K. S. Napol'skii, and A. R. Kaul, "Epitaxial calcium and strontium fluoride films on highly mismatched oxide and metal substrates by MOCVD: Texture and morphology," *Chem. Mater.*, vol. 22, pp. 175–185, 2010.
- [8] A. Makarevich, A. Shchukin, A. Markelov, S. Samoilenkov, P. Semyannikov, and N. Kuzmina, *Electrochem. Soc. Trans.*, vol. 25, pp. 525–532, 2009.
- [9] A. V. Markelov, S. V. Samoilenkov, A. R. Akbashev, A. L. Vasiliev, and A. R. Kaul, "Control of orientation of $\text{RbBa}_2\text{Cu}_3\text{O}_7$ films on substrates with low lattice mismatch via seed layer formation," *IEEE Trans. Appl. Supercond.*, vol. 21, pp. 3066–3069, 2011.
- [10] I. A. Rudnev, S. A. Pokrovskiy, and A. I. Podlivaev, *IEEE Trans. Appl. Supercond.*, vol. 22, p. 9001304, 2011.
- [11] E. D. Specht, A. Goyal, D. F. Lee, F. A. List, D. M. Kroeger, M. A. Paranthaman, R. K. Williams, and D. K. Christen, "Cube-textured nickel substrates for high-temperature superconductors," *Supercond. Sci. Technol.*, vol. 11, p. 945, 1998.
- [12] V. Matias, E. J. Rowley, Y. Coulter, B. Maiorov, T. Holesinger, C. Young, V. Glyantsev, and B. Moeckley, "YBCO films grown by reactive co-evaporation on simplified IBAD-MgO coated conductor templates," *Supercond. Sci. Technol.*, vol. 23, p. 014018, 2010.